Journal of Innovations in Business and Industry

Vol. 04, No. 01 (2026) 9-18, doi: 10.61552/JIBI.2026.01.002 - http://jibi.aspur.rs

DEVELOPMENT OF NATIONAL DIAGNOSTIC REFERENCE LEVELS FOR HEAD CT EXAMINATIONS IN MOROCCO: A CLINICAL INDICATION-BASED APPROACH TO OPTIMIZE RADIATION DOSE AND ENHANCE PATIENT SAFETY

Youssef Madkouri [1]
Hamza Sekkat
Youssef El Merabet
Mohammed Aggour
Farida Bentayeb
Abdellah Khallouqi

Received 12.10.2024.
Revised 17.12.2024.
Accepted 25.03.2025.

Keywords:

Clinical indication, DRLs, Head, Computed Tomography, Innovation, Morocco.

Original research

A B S T R A C T

This study investigates dosimetric data and technical parameters from 1,299 head CT examinations conducted across 20 hospitals, including 5 university, 8 provincial, and 7 private hospitals, using CT scanners from manufacturers such as Canon, General Electric, Siemens, and Hitachi. Various CT scanner configurations were employed, with technical parameters including kVp values ranging from 80 to 140, mAs between 100 and 300, and scan lengths varying from 6 cm to 28 cm. The dosimetric analysis revealed significant differences in radiation doses across clinical protocols. For stroke evaluation (364 patients) underwent non-contrast scans yielding a mean CTDIvol of 58.71 ± 3.20 mGy and a median effective dose of 12.33 ± 0.99 mSv. Acute brain protocols (272 patients) using similar scan parameters showed a mean CTDIvol of 55.66 ± 4.00 mGy and an effective dose of 11.69 ± 1.19 mSv. Post-contrast non-vascular brain scans (156 patients) resulted in a CTDIvol of 61.48 ± 4.50 mGy and an effective dose of 12.91 ± 1.33 mSv. Contrast-enhanced angiographic imaging (156 patients) with double-phase protocols recorded a mean CTDIvol of 57.60 ± 4.00 mGy and an effective dose of 12.09 ± 1.19 mSv. Oncology simulation scans (117 patients) required the highest doses, with a CTDIvol of 74.74 ± 15.69 mGy and an effective dose of 25.13 ± 1.80 mSv. In contrast,sinus protocols (130 patients) showed a lower mean CTDIvol of 50.08 ± 3.00 mGy and an effective dose of 9.82 ± 0.64 mSv, reflecting the reduced scan range. Temporal bone imaging (104 patients) employed a limited scan length, resulting in a lower CTDIvol of 49.71± 2.80 mGy and an effective dose of 5.57 ± 0.28 mSv. The study revealed significant variations in DRLs driven by clinical requirements and regional disparities in healthcare infrastructure.These findings highlight the balance between diagnostic accuracy and radiation dose optimization across different clinical indications, contributing to improved patient safety while maintaining clinical efficacy.

[1] Corresponding author: Youssef Madkouri
Email: youssef.madkouri@uit.ac.ma

1. INTRODUCTION

Computed tomography (CT) is a highly advanced medical imaging technique that combines X-ray and computer technology to create detailed cross-sectional images of the human body (Madkouri et al., 2025). Since the introduction of clinical CT scanners in 1972, there has been a notable rise in the number of CT scans performed on adults (Madkouri et al., 2023, Sekkat et al., 2024). CT scans deliver higher radiation doses than other imaging methods; in fact, a single CT scan can expose the body to radiation levels 150 to 1,100 times higher than those of a conventional X-ray, with doses ranging from 1 to 15 mSv (Poosiri et al., 2024) . Over time, high radiation doses can increase the risk of radiation-induced cancers (UNSCEAR, 2021). To minimize this risk, it is crucial to reduce patient exposure by optimizing CT scanning protocols.

Diagnostic Reference Levels (DRLs), introduced by the International Commission on Radiological Protection (ICRP) some years ago, have become an essential tool for optimizing radiation doses in diagnostic and interventional radiology and nuclear medicine (Paulo et al., 2020) . DRLs act as investigation thresholds to flag instances of unusually high radiation exposure, prompting a local review if they are consistently exceeded. Not intended for regulatory, commercial, or constraint purposes, DRLs instead serve as guidance to enhance patient safety without imposing formal dose limits (Damilakis et al., 2023).

In the European Union, the mandatory establishment and use of DRLs were implemented in 1997, with further emphasis added through the 2013 Council Directive 2013/59/EURATOM (BSSD), which calls for regular review and consistent application of DRLs in all Member States to improve health protection against the risks of ionizing radiation in medical exposure (European Society of Radiology (ESR), 2015).

Traditionally, DRLs have been based on anatomical locations across various imaging modalities. While this approach can be restrictive, particularly in computed tomography (CT), where different clinical indications for the same anatomical region often demand different protocols, each with distinct exposure requirements. For instance, head CT scans may be performed for various purposes, including for example the evaluation of acute stroke, cranial trauma, headaches and cerebral tumor detection. Each of these indications necessitates specific image quality parameters and scan lengths, which should be reflected in distinct diagnostic reference levels (DRLs). However, most international studies still define DRLs by anatomical location rather than clinical indication. Recently, some countries have begun to establish DRLs based on specific clinical indications (DRLci), and others are planning similar initiatives (Hassan et al., 2022; Paulo et al., 2020; Tsapaki et al., 2021) . In Morocco, however, no study has yet implemented DRLs based on clinical indications.

In this study, the dose descriptors used to define DRLs in CT include: volume computed tomography dose index (CTDIvol), which is the standard metric for estimating the radiation output of a CT scanner. This is calculated based on measurements obtained from a 16 cm or 32 cm phantom, with the unit expressed in milligray (mGy); and dose length product (DLP). This metric quantifies the total radiation dose used in a CT scan and is calculated as the product of CTDIvol (mGy) and scan length (cm), with the unit in mGy·cm (Madkouri et al., 2023). Both CTDIvol and DLP are essential for optimizing CT procedures. However, it's important to note that these descriptors reflect the output of the CT scanner and do not provide an estimate of the actual dose received by the patient (McCollough et al., 2011). On the other hand, the effective dose (E), which estimates the biological impact of radiation exposure on the human body. It is derived by multiplying the DLP by a conversion factor specific to the scanned body region, with the unit measured in millisieverts (mSv), provides a better estimate of the potential health risks by accounting for radiation sensitivity differences across tissues and organs (Goo, 2012).

Therefore, the aim of this study is to establish national diagnostic reference levels based on clinical indications (DRLci) and standard protocols in adult head CT procedures in Morocco. By focusing on clinical indications rather than solely anatomical locations, this study seeks to optimize radiation doses more effectively, customized to the specific diagnostic needs of each procedure.

2. MATERIALS AND METHODS

2.1. Data collection and technical parameters of standard protocol for head region

This study involved retrospective dosimetric data and axial images from 1,299 head CT examinations conducted across 20 hospitals, comprising 5 university hospitals (A), 8 provincial hospitals (B), and 7 private hospitals (C), utilizing various CT scanner systems from manufacturers including Canon (Japan), General Electric (USA), Siemens (Germany), and Hitachi (Japan). The scanners employed different configurations, with the CT Aquilion Prime and CT Aquilion RXL/Alexion (Canon) used in all university, provincial and private hospitals, featuring 80 and 16 detector rows respectively, a kVp of 120, and varying mA values (250 and 200, respectively). These scanners utilized AIDR 3D (Adaptive Iterative Dose Reduction 3D) and had rotation times of 0.75 seconds. The CT Brightspeed Optima 520 CT (General Electric) system are in use at university and provincial hospitals had 16 detector rows, a kVp of 120, and a mA of 250, with ASIR (Adaptive Statistical Iterative Reconstruction), a rotation time of 0.8 seconds, and collimation of 16x1.25 mm. The Discovery CT750 HD (General Electric) in university hospitals, with 64 detector rows, a kVp of 120, and 250 mA, used ASIR

reconstruction, with rotation times of 0.8 seconds and a collimation of 64x0.625 mm. The Siemens CT SOMATOM Scope VC28 and Sensation systems, located in university and private hospitals, featured 16 and 64 detector rows respectively, with 130 kVp, 240 mA, and ADMIRE (Advanced Modeled Iterative Reconstruction), and a rotation time of 0.6 seconds. The Hitachi Supria and Scenaria CT scanners in provincial and private hospitals had 16 and 64 detector rows, with 140 kVp, 300 mA, and Intelli IP (Intelligent Iterative Reconstruction), with rotation times ranging from 0.75 to 1 second and collimation of 16x1.25 mm and 64x0.625 mm. All scanners followed standard protocols based on their manufacturer specifications, ensuring consistent image quality and radiation dose across the different hospital settings (Table. 1). The kVp and mAs presented in the present section concern the pre-defined standard protocol of head region in CT examination and does not cover the full protocols routinely used. These parameters will be used in results analysis in order to compare between the different indications associated to their appropriate protocols.

Table 1. Technical parameters of CT examination for head region across manufacturers

Manufacturer System	Hospital type	Detector rows	Rotation time (s)	Collimation (mm)	Slice thickness (mm)	Pitch	Reconstruction process
CT Aquilion Prime (Canon, Japan)	(B,C)	80	0.75	80x0.5	1	0.969	AIDR 3D
CT Aquilion RXL,CT Alexion (Canon, Japan)	(A,2B,C)	16	0.75	16x1	1	0.969	AIDR 3D
CT Brightspeed, Optima 520 CT (General Electric, USA)	(A,B)	16	0.8	16x1.25	1.25	0.938	ASIR
Discovery CT750 HD (General Electric, USA)	(2A)	64	0.8	64x0.625	1.25	0.969	ASIR
CT SOMATOM Scope CT VC28 (Siemens, Germany)	(C)	16	0.6	16x1.5	1.5	0.8	ADMIRE
CT Sensation (Siemens, Germany)	(A,C)	64	0.6	64x0.6	1	0.8	ADMIRE
CT Hitachi Supria (Hitachi, Japan)	(4B,2C)	16	1	16x1.25	1.25	0.57	Intelli IP (4)
CT Scenaria (Hitachi, Japan)	(C)	64	0.75	64x0.625	1.25	0.969	Intelli IP (4)

For oncology simulations, a higher field of view (FOV) and scan length are often employed to assess tumor involvement in regions such as the nasopharynx (cavum), when the cancer has developed in the subclavian lymph nodes by extending the scan range from the skull base to the upper chest (Figure 1(A)), extending beyond the standard FOV used for routine head CT (Figure 1(B)).

The CT imaging protocols for the sinus and temporal bone are tailored to specific clinical indications, such as sinusitis, nasal obstruction, nasal septal abnormalities, polyposis, facial pain, otosclerosis, otitis media, mastoiditis, trauma, or evaluating implants and cholesteatomas. These protocols typically employ a smaller field of view (FOV) and short scan length compared to standard protocol, minimizing the irradiated volume. For these applications, thin-slice thicknesses and high-resolution bone reconstructions are often used to ensure detailed visualization of the fine osseous structures while optimizing patient safety. This targeted approach aligns with the ALARA (As Low As Reasonably Achievable) principle in radiation protection, prioritizing diagnostic quality with minimal exposure (Strauss & Kaste, 2006; Yeung, 2019).

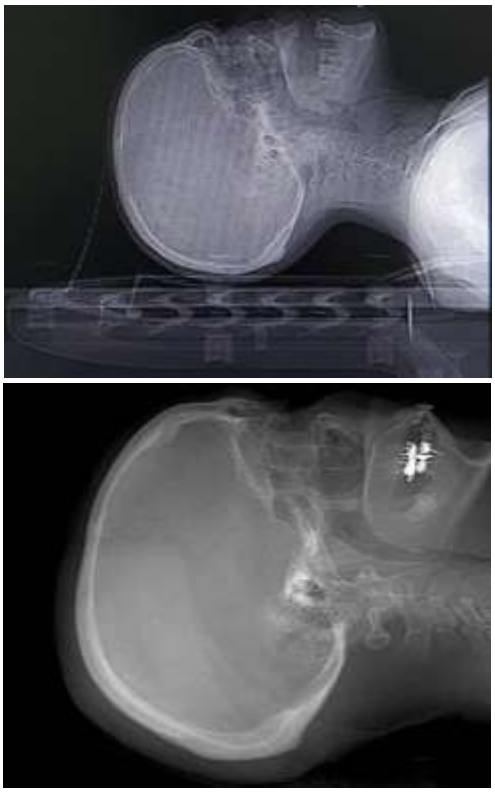

(a) (b)

Figure 1. (a) CT oncology simulation head protocol with extended FOV; (b) Standard protocol of adult head CT examination

2.2. Clinical indications of head-based protocols

The seven indication-based CT protocols, listed in decreasing frequency as shown in Figure 2, were developed to address the most commonly performed examinations while ensuring optimal clinical utility and dose efficiency. The stroke protocol focuses on rapid assessment of ischemic or hemorrhagic events to guide urgent interventions, followed by the acute brain protocol for neurological emergencies such as trauma, seizures, or altered mental states. The non-vascular brain protocol evaluates structural abnormalities, including tumors and infections, while the angiography protocol provides detailed vascular imaging for conditions like aneurysms or arteriovenous malformations.

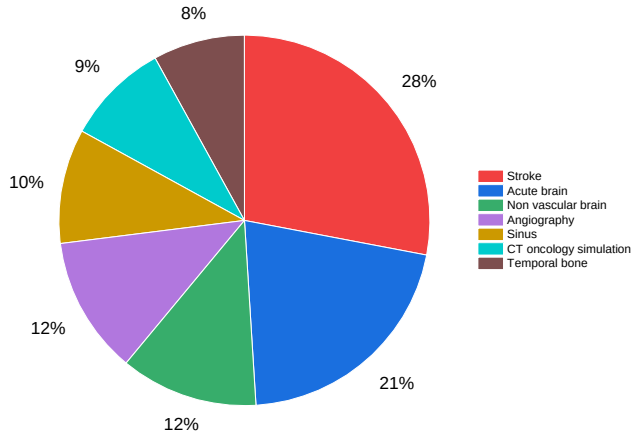

Figure 2. Distribution of indication-based ct protocols by frequency

The sinus protocol targets sinus-related pathologies, the CT oncology simulation protocol supports precise radiotherapy planning, and the temporal bone protocol addresses conditions affecting hearing and the inner ear. Each protocol is designed to balance diagnostic accuracy with radiation dose optimization, reflecting the clinical priorities of high-demand examinations.

3. RESULTS

The study analyzed various CT protocols and their clinical applications across a diverse patient cohort as presented in Table 2. For stroke evaluation, non-contrast scans at 120-140 kVp and 250-300 mAs were utilized in 364 patients to identify hemorrhagic events. Similarly, acute brain protocols targeting cranial trauma and neurological symptoms used identical scan settings in 272 patients. Post-contrast scans for non-vascular brain conditions, including metastatic disease, tumor control, and abscess evaluation, employed 100-120 kVp and 220-250 mAs in 156 patients. Angiographic imaging for ischemic stroke, infectious abnormalities, arteriovenous malformations, and aneurysms was conducted using a double-phase contrast protocol with 100-120 kVp and 200-250 mAs in the first phase, followed by 120-130 kVp and 200-230 mAs in the second phase, involving 156 patients. Non-contrast sinus scans, addressing conditions such as sinusitis and trauma, were performed at 80-110 kVp and 100-180 mAs for 130 patients. CT oncology simulation protocols, both with and without contrast, assessed tumor volumes and locations at 100-120 kVp and 200-250 mAs in 117 patients. Finally, temporal bone imaging for conditions like cholesteatoma and otitis media employed non-contrast scans at 100-120 kVp and 150-200 mAs in 104 patients. These protocols put attention to the specificity of CT imaging for distinct clinical indications and patient needs.

Table 2. Summary of national protocols with their clinical indications, scan parameters (range) and patient distribution

Protocol	Scan type	Clinical indication	kVp	mAs	Scan length (cm)	Number of patients
Stroke	Non-contrast scan	Evaluation of hemorrhagic stroke	120-140	250-300	14-20	364
Acute brain	Non-contrast scan	Cranial trauma and neurological symptoms	120-140	250-300	15-18	272
Non vascular brain	Post-contrast scan	Metastatic disease and tumor control / abscess	100-120	220-250	15-20	156
Angiography	Contrast scan (Double phase)	Evaluation of ischemic stroke / assessment of infectious abnormalities / arteriovenous malformation / neurysms	1st phase: 100-120 2nd phase: 120-130	1st phase: 200-250 2nd phase: 200-230	15-18	156
Sinus	Non contrast scan	Sinusitis / nasal septal / trauma	80-110	100-180	14-16	130
CT oncology simulation	Non contrast scan / Contrast scan	Assessment of tumor volume and location	100-120	200-250	20-28	117
Temporal bone	Non contrast scan	Cholesteatoma/ otitis media	100-120	150-200	6-10	104

The dosimetric analysis of various CT protocols in Table 3 shows differences in radiation doses, reflecting the specific clinical indications and corresponding technical parameters. For evaluation of hemorrhagic stroke, a scan length of 14–20 cm, kVp ranging from 120–140, and mAs between 250–300 were employed for 364 patients. The mean CTDIvol was 58.71 ± 3.20 mGy, with a median of 56.00 mGy (range: 50.00–60.00 mGy), while the DLP averaged 880.74 ± 70.50 mGy·cm, and the median effective dose (E) was 12.33 ± 0.99 mSv. These relatively high doses stem from the need for optimal image quality to identify subtle intracranial hemorrhages, which require precise contrast differentiation. For cranial trauma and neurological symptoms, a similar scan length of 15–18 cm was applied for 272 patients using 120–140 kVp and 250–300 mAs. The mean CTDIvol was 55.66 ± 4.00 mGy (median: 56.20 mGy), with a DLP of 834.90 ± 85.40 mGy·cm and an effective dose of 11.69 ± 1.19 mSv. These parameters balance adequate image resolution to detect skull fractures or traumatic intracranial abnormalities while maintaining a reasonable radiation dose.

In cases of metastatic disease, tumor control, or abscess evaluation, post-contrast scans used 100–120 kVp and 220–250 mAs over a scan length of 15–20 cm for 156 patients. The CTDIvol was higher at 61.48 ± 4.50 mGy (median: 57.70 mGy), with a DLP of 922.20 ± 95.20 mGy·cm and an effective dose of 12.91 ± 1.33 mSv. The elevated doses are justified by the need for enhanced visualization of contrast-avid lesions to precisely assess metastatic deposits or abscess formations. For evaluation of ischemic stroke, infectious abnormalities, arteriovenous malformations, or aneurysms, a contrast-enhanced angiographic protocol with a double-phase technique was used, involving 100–120 kVp and 200–250 mAs in the first phase, followed by 120–130 kVp and 200–230 mAs in the second phase, covering a scan length of 15–18 cm for 156 patients. The mean CTDIvol was 57.60 ± 4.00 mGy (median: 57.60 mGy), with a DLP of 864.00 ± 85.00 mGy·cm and an effective dose of 12.09 ± 1.19 mSv. The two-phase protocol ensures detailed visualization of vascular anatomy and pathologies, such as arterial occlusions or aneurysmal dilations, critical for treatment planning.

For sinusitis, nasal septal evaluation, or trauma, a non-contrast protocol was used with a scan length of 14–16 cm, 80–110 kVp, and 100–180 mAs for 130 patients. The CTDIvol averaged 50.08 ± 3.00 mGy (median: 49.80 mGy), with a DLP of 701.12 ± 45.70 mGy·cm and an effective dose of 9.82 ± 0.64 mSv. These lower values reflect the reduced anatomical complexity and smaller scan range required for sinus imaging.

In tumor volume and location assessments, including CT oncology simulation, the protocol involved both non-contrast and contrast-enhanced scans with 100–120 kVp and 200–250 mAs, spanning 20–28 cm for 117 patients. The mean CTDIvol was significantly higher at 74.74 ± 15.69 mGy (median: 79.00 mGy), with a DLP of 1794.80 ± 128.77 mGy·cm and an effective dose of 25.13 ± 1.80 mSv. The higher doses are essential for comprehensive tumor mapping and treatment planning, necessitating large scan lengths and high-resolution imaging. Finally, for temporal bone imaging (cholesteatoma/otitis media), non-contrast scans used 100–120 kVp and 150–200 mAs over a limited scan length of 6–10 cm for 104 patients. The mean CTDIvol was 49.71 ± 2.80 mGy (median: 47.00 mGy), with a DLP of 398.36 ± 20.30 mGy·cm and an effective dose of 5.57 ± 0.28 mSv. These protocols focus on high spatial resolution at lower radiation doses to visualize the fine osseous structures of the temporal bone.

Table 3. Diagnostic reference levels of CT protocols for the various national clinical indications: mean, median, range (Min-Max) and third quartile values for $CTDI_{vol}$, DLP and effective dose (E)

Dosimetric quantity	**CTDIvol (mGy)**				**DLP (mGy.cm)**				**E (mSv)**			
Indication	Mean	Median	Min-Max	3rd Quartile	Mean	Median	Min-Max	3rd Quartile	Mean	Median	Min-Max	3rd Quartile
Evaluation of hemorrhagic stroke	58.71 ± 3.20	56.00	50.00-60.00	58.50	880.74 ± 70.50	992.00	715.00-1100.00	927.23	12.33 ± 0.99	13.84	10.01-15.40	12.99
Cranial trauma and neurological symptoms	55.66 ± 4.00	56.20	50.70-60.00	58.00	834.90 ± 85.40	956.30	761.00-1080.00	891.22	11.69 ± 1.19	13.39	10.65-15.12	12.47
Metastatic disease and tumor control / abscess	61.48 ± 4.50	57.70	55.00-68.60	63.50	922.20 ± 95.20	1203.80	825.00-1400.00	985.98	12.91 ± 1.33	16.85	11.55-19.60	13.80
Evaluation of ischemic stroke / assessment of infectious abnormalities / arteriovenous malformation / neurysms	57.60 ± 4.00	57.60	50.00-63.00	60.00	864.00 ± 85.00	1095	750.00-1250.00	920.95	12.09 ± 1.19	15.33	10.50-17.50	12.89

Sinusitis / nasal septal / trauma	50.08 ± 3.00	49,80	42.00-48.50	47.00	701.12 ± 45.70	785.00	588.00-780.00	731.74	9.82 ± 0.64	10.99	8.23-12.32	10.24
Assessment of tumor volume and location	74.74 ± 15.69	79.00	64.05-90.43	85.33	1794.80 ±128.77	2278.00	1298.00-2340.00	1881.08	25.13 ± 1.80	31.89	18.17-32.76	26.34
Cholesteatoma/ otitis media	49.71 ± 2.80	47.00	45.50-55.00	51.50	398.36 ± 20.30	415.00	272.00-555.00	412.00	5.57 ± 0.28	5.81	3.80-7.77	5.77

The variations in the mean DLP across various cities in Morocco highlight significant regional differences in diagnostic radiation exposure as shown in Figure 3. Cities like Agadir (~2211 mGy·cm) and Al Hoceima (~2204 mGy·cm) report the highest DLP values, which is attributed to the fact that the hospitals in these areas, from which data was retrospectively collected, are oncology centers. These centers likely perform higher-dose imaging procedures for cancer patients due to the higher FOV used as previously explained (Figure 1). Other cities such as Sidi Slimane (~1609 mGy·cm), Oujda (~1395 mGy·cm) exhibit moderate DLP values, while cities like Rabat (~804 mGy·cm) and Dakhla (~790 mGy·cm) present lower radiation exposure levels. The wide range of DLP values shows the disparities in medical imaging protocols and patient demographics across the country. This variation in DLP values provides an essential context for understanding the role of healthcare infrastructure in influencing radiation exposure in diagnostic imaging across Morocco.

The comparison of DRLs in terms of DLP for stroke clinical indications resulted in notable variations across different studies (Figure 4). Tsapaki et al. (2021) reported the highest DLP (1386 mGy·cm) (Tsapaki et al., 2021), followed by Oldenburg et al. (2020) (1076 mGy·cm)(Oldenburg et al., 2020) and Habib Geryes et al. (2019) (1010 mGy·cm)(Habib Geryes et al., 2019) and Shrimpton et al. (2014) also reporting 970 mGy·cm (Shrimpton et al.,2014), while the present study demonstrated a relatively lower DLP of 880.74 mGy·cm. The European Commission and Ireland provided comparable DRLs of 807 mGy·cm and 857 mGy·cm, respectively (European Commission. Directorate General for Energy, 2021; Foley et al., 2012). Tan et al. showed the lowest DLP among the compared studies (626 mGy·cm) (Tan et al., 2023). Notably, the comparison in this paper focused on stroke clinical indications because other studies were limited to one or two specific indications, such as stroke and/or sinusitis. In contrast, our study is comprehensive, targeting the head region and encompassing all associated clinical indications on a nationwide scale in Morocco. This broader focus provides a more profound and representative assessment of DRLs within the national context.

Figure 3. Geographical distribution of cities in morocco with color-coded diagnostic reference levels in terms of DLP

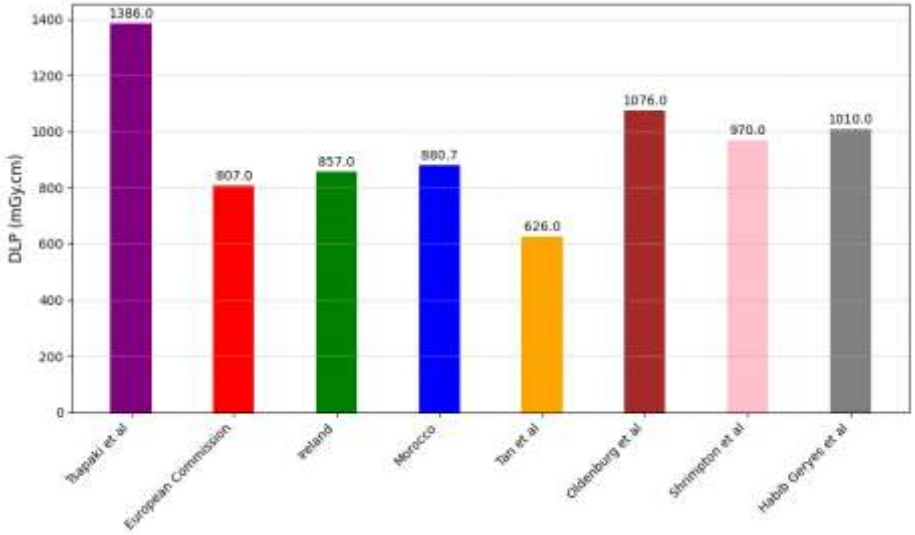

Figure 4. Comparison of national DRLS based on stroke clinical indication with other studies

4. DISCUSSION

This is the first study to present nationwide, large-scale results for DRLs in head CT examinations based on clinical indications in Morocco. These findings provide a comprehensive baseline for comparison with local radiological practices and can serve as valuable guidelines for institutions aiming to establish their own local DRLs. Unlike previous studies in Morocco, which primarily focused on general and limited anatomical-based DRLs (Benmessaoud et al., 2021; El Mansouri et al., 2022; Semghouli et al. 2017). This study offers a detailed analysis specific to the head region and its associated clinical indications. This approach not only enhances the understanding of current practices but also supports efforts to optimize radiation doses while maintaining diagnostic quality in a personalized approach for each clinical indication.

In two sites located in Rabat and Dakhla, equipped with an Aquilion Prime 80 CT scanner, the stroke and temporal bone protocols utilized the volume acquisition mode. This acquisition mode significantly contributed to lower dose-length product (DLP) values compared to many other sites that employed helical CT acquisition mode. The reduction in DLP achieved with volume acquisition is consistent with findings from previous studies, which have demonstrated its advantages in dose optimization (Madkouri et al., 2023). Volume acquisition mode is inherently more efficient in minimizing overlapping exposures and improving dose distribution, particularly in targeted examinations such as those for the stroke and temporal bone. These findings highlight the potential benefits of adopting advanced acquisition techniques in reducing radiation exposure without compromising diagnostic quality. Incorporating such protocols into routine practice, where appropriate, could help standardize dose optimization strategies across different sites, further supporting the establishment of robust, indication-specific DRLs. This underscores the need for continuous training and protocol standardization in the implementation of modern CT technologies across healthcare facilities as shown in Figure 3.

For sinus CT protocols, the specific clinical objectives can significantly influence the required dose. For example, when medical radiologists aim to evaluate not only the bony structures but also the surrounding soft tissues, a higher dose is typically necessary to ensure adequate image quality and diagnostic accuracy, which represented the case of some sites. This increased dose requirement stems from the need for finer contrast resolution to differentiate soft tissue details, such as mucosal thickening, masses, or other pathological changes, which are less conspicuous at lower doses optimized solely for bone visualization. Conversely, protocols designed exclusively for bone assessment, such as detecting fractures or bony erosions, can operate at lower doses since the higher contrast between bone and air requires less radiographic intensity (Al Abduwani et al., 2016).

In Morocco, many imaging centers still rely on helical 16-detector row CT scanners for brain imaging, which require longer scan times and higher radiation doses compared to more advanced volumetric systems. Technologies such as wide-volume acquisitions and flash modes, available in larger detector arrays like 80-, 128-, 256- or 320-detector row systems, significantly improve dose efficiency and image quality by covering larger volumes in a single rotation, thus minimizing overlapping exposures. These innovations reduce radiation dose while maintaining diagnostic accuracy (Garba et al., 2022; Jeon et al., 2018). This situation underscores the importance of protocol optimization and the adoption of modern equipment where feasible. While upgrading to higher detector row CT systems would represent a significant investment, it would align with global trends in dose reduction and enhance compliance with international diagnostic reference levels (DRLs). Furthermore, focusing on training radiologists and technologists to optimize protocols on existing systems could mitigate some of the dose disparities associated with older scanner technologies, ensuring patient safety while maintaining diagnostic quality.

The CT angiography, a critical diagnostic procedure used to visualize blood vessels and assess conditions such as aneurysms, stenosis, and blockages, typically involves two distinct acquisition phases: the pre-contrast phase and the contrast-enhanced phase (Chhetri & Thapa, 2020) . This two-phase approach significantly increases the radiation exposure to patients compared to other CT protocols, which often require only a single acquisition phase. The pre-contrast phase is necessary to capture baseline anatomical details, while the contrast-enhanced phase allows for the visualization of vascular structures after the administration of a contrast agent. Each phase requires a separate scan, contributing to cumulative radiation doses. The use of high contrast in blood vessels relative to surrounding tissues necessitates high radiation doses to ensure optimal visualization, especially when capturing dynamic processes or smaller vessels in the head protocol. Moreover, the lengthy nature of angiographic procedures, coupled with the need for multiple phases of data acquisition, further amplifies the total radiation burden. This increased radiation dose for angiography highlights the need for strict protocol optimization to minimize unnecessary exposure. Advanced technologies, such as iterative reconstruction techniques and automated dose modulation, are crucial in reducing radiation levels while maintaining diagnostic quality (Araki et al., 2024). Additionally, the careful selection of imaging parameters based on patient size, clinical indication, and diagnostic requirements can help balance the need for high-quality angiographic images with the goal of minimizing patient radiation exposure.

In the case of temporal bone CT scans, the use of a small field of view (FOV), typically ranging from 6 to 10 cm, plays a crucial role in reducing radiation exposure (Madkouri et al., 2023). By limiting the scanned area to the region of interest, this focused approach significantly minimizes the amount of irradiated tissue compared to

scans with larger FOVs, such as those used for other head examinations. The smaller FOV allows for a more targeted examination, which not only enhances image resolution but also reduces the total radiation dose delivered to the patient (Strauss & Kaste, 2006). The reduced irradiation is particularly beneficial in procedures like temporal bone CT, where high-resolution images of the bony structures of the ear, including the cochlea, ossicles, and auditory canal, are essential for diagnostic accuracy. The smaller FOV ensures that only the relevant anatomy is exposed to radiation, preserving surrounding tissues and limiting unnecessary dose to non-target areas.

The use of a higher field of view (FOV) and extended scan lengths in CT oncology simulations represents a significant deviation from standard head CT protocols, tailored to the clinical needs of cancer patients. These adjustments are particularly crucial when assessing tumor involvement in the nasopharynx (cavum) and subclavian lymph nodes (Legmouz et al., 2022; Sebelego et al., 2024). By extending the scan range from the skull base to the upper chest, comprehensive visualization of tumor spread and lymphatic involvement is achieved, facilitating accurate staging and treatment planning. The inclusion of extended scan lengths ensures that critical anatomical regions, often omitted in routine head CT scans, are thoroughly evaluated. This approach is especially relevant for patients undergoing radiotherapy, where precise dose calculations and organ protection are essential, such as the optic chiasm and optic nerves, are highly radiosensitive, and exceeding recommended dose thresholds could lead to severe complications. By incorporating these organs into the imaging field, clinicians can better evaluate the dose distribution and implement strategies to safeguard these critical structures (Ritthipravat et al., 2008). The application of intravenous contrast further enhances the delineation of tumor margins and lymph nodes, improving diagnostic accuracy (Ding et al., 2021). However, these extended protocols necessitate careful consideration of radiation exposure, highlighting the importance of balancing diagnostic requirements with patient safety. This aligns with the development of diagnostic reference levels (DRLs) tailored to clinical indications, ensuring that imaging practices adhere to radiation protection principles without compromising diagnostic outcomes. Incorporating these optimized protocols into routine practice can significantly improve the management of oncology patients, providing a comprehensive framework for diagnosis, treatment planning, and dose optimization. Further studies should investigate the long-term impact of such tailored protocols on patient outcomes and their integration into national and international guidelines for head CT examinations.

5. CONCLUSION

In conclusion, establishing DRLs based on clinical indications provides a more tailored and accurate framework for optimizing radiation doses in CT imaging. This approach ensures that dose benchmarks are aligned with specific diagnostic requirements, enhancing both patient safety and image quality. By addressing clinical indication-specific DRLs, as demonstrated in this study, healthcare providers can better standardize practices, identify areas for dose optimization, and support the development of guidelines that reflect real-world clinical scenarios. This methodology represents a significant step forward in advancing radiological safety and quality of diagnosis

Acknowledgment: All data and images are collected with full consent of involved parties, following all domestic and international ethical standards and ethics approval.

.

References:

Al Abduwani, J., ZilinSkiene, L., Colley, S., & Ahmed, S. (2016). Cone beam CT paranasal sinuses versus standard multidetector and low dose multidetector CT studies. *American Journal of Otolaryngology*, 37(1), 59–64. DOI: 10.1016/j.amjoto.2015.08.002

Araki, S., Nakamura, S., Takafuji, M., Ichikawa, Y., Sakuma, H., & Kitagawa, K. (2024). Ultra-low-dose coronary computed tomography angiography using photon-counting detector computed tomography. *European Heart Journal - Imaging Methods and Practice*, 2(3), 125. DOI: 10.1093/ehjimp/qyae125

Benmessaoud, M., Housni, A., Elmabrouki, M., Essasnaoui, F., Sadiki, N., Dadouch, A., & Labzour, A. (2021). Derivation Of Local Diagnostic Reference Levels For Common Adult Computed Tomography Examinations In Moroccan Hospital. *Radiation Protection Dosimetry*, 194(4), 208–213. DOI: 10.1093/rpd/ncab095

Chhetri, P. K., & Thapa, K. (2020). CT Angiography in Patients with Peripheral Arterial Disease. *Journal of College of Medical Sciences-Nepal*, 16(2), 78–82. DOI: 10.3126/jcmsn.v16i2.28655

Damilakis, J., Frija, G., Brkljacic, B., Vano, E., Loose, R., Paulo, G., Brat, H., Tsapaki, V., & the European Society of Radiology. (2023). How to establish and use local diagnostic reference levels: An ESR EuroSafe Imaging expert statement. *Insights into Imaging*, 14(1), 27. DOI: 10.1186/s13244-023-01369-x

Ding, Z., Deng, C., Wang, Z., Liu, L., Ma, X., Huang, J., Wang, X., Xuan, M., & Xie, H. (2021). Comparison of contrast-enhanced ultrasound and contrast-enhanced computed tomography for the diagnosis of cervical lymph node metastasis in squamous cell carcinoma of the oral cavity. *International Journal of Oral and Maxillofacial Surgery*, 50(3), 294–301. DOI: 10.1016/j.ijom.2020.07.013

El Mansouri, M., Talbi, M., Choukri, A., Nhila, O., & Aabid, M. (2022). Establishing local diagnostic reference levels for adult computed tomography in Morocco. *Radioprotection*, 57(1), 61–66. DOI: 10.1051/radiopro/2021035

European Commission. Directorate General for Energy. (2021). European study on clinical diagnostic reference levels for X-ray medical imaging: EUCLID. Publications Office. https://data.europa.eu/doi/10.2833/452154

European Society of Radiology (ESR). (2015). Summary of the European Directive 2013/59/Euratom: Essentials for health professionals in radiology. *Insights into Imaging*, 6(4), 411–417. DOI: 10.1007/s13244-015-0410-4

Foley, S. J., McEntee, M. F., & Rainford, L. A. (2012). Establishment of CT diagnostic reference levels in Ireland. *The British Journal of Radiology*, 85(1018), 1390–1397. DOI: 10.1259/bjr/15839549

Garba, I., Fatima, A. M., Abba, M., Yakubu, M., Mansur, Y., Lawal, Y., Abubakar, A., & Usman, A. U. (2022). Analysis of image quality and radiation dose in routine adult brain helical and wide-volume computed tomography procedures. *Journal of Medical Imaging and Radiation Sciences*, 53(3), 429–436. DOI: 10.1016/j.jmir.2022.05.008

Goo, H. W. (2012). CT Radiation Dose Optimization and Estimation: An Update for Radiologists. *Korean Journal of Radiology*, 13(1), 1. DOI: 10.3348/kjr.2012.13.1.1

Habib Geryes, B., Hornbeck, A., Jarrige, V., Pierrat, N., Ducou Le Pointe, H., & Dreuil, S. (2019). Patient dose evaluation in computed tomography: A French national study based on clinical indications. *Physica Medica*, 61, 18–27. DOI: 10.1016/j.ejmp.2019.04.004

Hassan, N. H., Osman, N. D., Mohd Daud, N., & Mockter, T. (2022). The Determination of Diagnostic Reference Range (DRR) Based on Clinical Indications in Head Computed Tomography (CT) Imaging. *Asian Journal of Medicine and Biomedicine*, 6(S1), 48–49. DOI: 10.37231/ajmb.2022.6.S1.523

Jeon, S. K., Choi, Y. H., Cheon, J.-E., Kim, W. S., Cho, Y. J., Ha, J. Y., Lee, S. H., Hyun, H., & Kim, I.-O. (2018). Unenhanced 320-row multidetector computed tomography of the brain in children: Comparison of image quality and radiation dose among wide-volume, one-shot volume, and helical scan modes. *Pediatric Radiology*, 48(4), 594–601. DOI: 10.1007/s00247-017-4060-1

Legmouz, M., El Ouahabi, A., Boulbaroud, S., & Azzaoui, F. Z. (2022). Brain tumors among Moroccan adolescents in the region of Rabat-Sale-Kenitra, Morocco. *Acta Neuropsychologica*, 20(3), 345–353. DOI: 10.5604/01.3001.0016.0760

Madkouri, Y., Aggour, M., Bouzekraoui, Y., & Bentayeb, F. (2023). Radiation Dose Optimization during Temporal Bone CT Examination Using One-Shot Axial Volumetric Acquisition. *Iranian Journal of Medical Physics, 20*(4), 215 DOI: 10.22038/ijmp.2022.63627.2087

Madkouri, Y., Sekkat, H., El Merabet, Y., Talbi, M., Aggour, M., Bentayeb, F., & Khallouqi, A. (2025). Helical to wide volume acquisition in lumbar spine CT: Structures scoring based analysis. *Radiation Physics and Chemistry*, 226, 112214. DOI: 10.1016/j.radphyschem.2024.112214

McCollough, C. H., Leng, S., Yu, L., Cody, D. D., Boone, J. M., & McNitt-Gray, M. F. (2011). CT Dose Index and Patient Dose: They Are Not the Same Thing. Radiology, 259(2), 311–316. DOI: 10.1148/radiol.11101800

Oldenburg D, Yu S, Luong J (2020). Diagnostic Reference Levels and Achievable Doses for Computed Tomography for EUCLID (European Study on Clinical DRLs) Defined Clinical Indications: Data from a Multinational Dose Registry. Radiological Society of North America 2019 Scientific Assembly and Annual Meeting, December 1 - December 6, 2019, Chicago IL. http://archive.rsna.org/2019/19006658.html Last assessed 15th Nov 2020

Paulo, G., Damilakis, J., Tsapaki, V., Schegerer, A. A., Repussard, J., Jaschke, W., Frija, G., European Society of Radiology, Hierath, M., & Clark, J. (2020). Diagnostic Reference Levels based on clinical indications in computed tomography: A literature review. *Insights into Imaging*, 11(1), 96. DOI: 10.1186/s13244-020-00899-y

Poosiri, S., Krisanachinda, A., & Khamwan, K. (2024). Evaluation of patient radiation dose and risk of cancer from CT examinations. Radiological Physics and Technology, 17(1), 176–185. DOI: 10.1007/s12194-023-00763-w

Ritthipravat, P., Tatanun, C., Bhongmakapat, T., & Tuntiyatorn, L. (2008). Automatic Segmentation of Nasopharyngeal Carcinoma from CT Images. 2008 International Conference on BioMedical Engineering and Informatics, 18–22. DOI: 10.1109/BMEI.2008.236

Sebelego, I.-K., Acho, S., & Rae, W. I. D. (2024). Clinical diagnostic reference levels and image quality metrics for CT in oncology patients. *South African Journal of Radiology*, 28(1), 2960. DOI: 10.4102/sajr.v28i1.2960

Sekkat, H., Madkouri, Y., Khallouqi, A., & El Rhazouani, O. (2024). Risk Management and Failure Analysis in Diagnostic X-ray Equipment: A Comprehensive Analysis and Novel Approaches for Failure Prevention and System Reliability. *Journal of Failure Analysis and Prevention*, 24(5), 2327–2340. DOI: 10.1007/s11668-024-02025-2

Shrimpton PC, Hillier MC, Meeson S, Golding SJ (2014) Doses & from computed tomography (CT) examinations in the UK – 2011. (n.d.). Doses from computed tomography (CT) examinations in the UK – 2011 Review Public Health England.

Semghouli, S., Amaoui, B., Kharras, A. E., Bouyakhlef, K., Hakam, O., & Choukri, A. (2017). Establishment of a diagnostic reference level for brain CT procedures in Moroccan Hospitals. *International Journal of Advanced Research*, 5(5), 319-324.

Strauss, K. J., & Kaste, S. C. (2006). The ALARA (as low as reasonably achievable) concept in pediatric interventional and fluoroscopic imaging: Striving to keep radiation doses as low as possible during fluoroscopy of pediatric patients—a white paper executive summary. *Pediatric Radiology*, 36(S2), 110. DOI: 10.1007/s00247-006-0184-4

Tan, W. S., Foley, S., & Ryan, M. L. (2023). Investigating CT head diagnostic reference levels based on indication-based protocols – a single site study. *Radiography*, 29(4), 786–791. DOI: 10.1016/j.radi.2023.05.003

Tsapaki, V., Damilakis, J., Paulo, G., Schegerer, A. A., Repussard, J., Jaschke, W., & Frija, G. (2021). CT diagnostic reference levels based on clinical indications: Results of a large-scale European survey. *European Radiology*, 31(7), 4459–4469. DOI: 10.1007/s00330-020-07652-5

UNSCEAR. (2021). Unies, N. (1969). Rapport du Comité scientifique des Nations Unies pour l'étude des effets des rayonnements ionisants. Nations Unies.

Yeung, A. W. K. (2019). The "As Low As Reasonably Achievable" (ALARA) principle: A brief historical overview and a bibliometric analysis of the most cited publications. *Radioprotection*, 54(2), 103–109. DOI: 10.1051/radiopro/2019016

Youssef Madkouri
Laboratory of Electronic Systems, Information Processing, Mechanics and Energetics, Faculty of Sciences, University Ibn Tofail , Kenitra, Morocco
youssef.madkouri@uit.ac.ma
ORCID: 0000-0002-5030-7444

Hamza Sekkat
Laboratory of Health Sciences and Technologies, Higher Institute of Health Sciences, Settat, Morocco

Youssef El Merabet
Laboratory of Electronic Systems, Information Processing, Mechanics and Energetics, Faculty of Sciences, University Ibn Tofail , Kenitra, Morocco
youssef.madkouri@uit.ac.ma
ORCID: 0000-0003-0771-4674

Mohammed Aggour
Laboratory of Electronic Systems, Information Processing, Mechanics and Energetics, Faculty of Sciences, University Ibn Tofail , Kenitra, Morocco
youssef.madkouri@uit.ac.ma
ORCID: 0000-0001-5801-1958

Farida Bentayeb
Laboratory of High Energy Physics, Modelling and Simulation, Faculty of Science, Mohammed V Agdal University, Rabat, Morocco
ORCID: 0000-0003-2773-8016

Abdellah Khallouqi
Laboratory of Health Sciences and Technologies, Higher Institute of Health Sciences, Settat, Morocco
ORCID: 0009-0008-5050-748X